CORA Cork Open Research Archive
Cartlann Taighde Oscailte Chorcaí

| | |
|---|---|
| Title | Guanidine functionalized porous SiO2 as heterogeneous catalysts for microwave depolymerization of PET and PLA |
| Authors | Casey, Éadaoin;Breen, Rachel;Pareras, Gerard;Rimola, Albert;Holmes, Justin D.;Collins, Gillian |
| Publication date | 2024-03-06 |
| Original Citation | Casey, É., Breen, R., Pareras, G., Rimola, A., Holmes, J. D. and Collins, G. (2024) 'Guanidine functionalized porous SiO 2 as heterogeneous catalysts for microwave depolymerization of PET and PLA', RSC Sustainability, 2(4), pp.1040-1051. Available at: https://doi.org/10.1039/D3SU00425B |
| Type of publication | Article (peer-reviewed) |
| Link to publisher's version | 10.1039/D3SU00425B |
| Rights | © 2024, the Authors. Published by the Royal Society of Chemistry. This open access article is made available under the CC BY-NC license (https://creativecommons.org/licenses/by-nc/4.0/) - https://creativecommons.org/licenses/by-nc/4.0/ |
| Download date | 2026-11-15 15:25:40 |
| Item downloaded from | https://hdl.handle.net/10468/15872 |

UCC
University College Cork, Ireland
Coláiste na hOllscoile Corcaigh

Electronic Supplementary Material (ESI) for RSC Sustainability.
This journal is © The Royal Society of Chemistry 2024

# Supplementary Information

# Guanidine Functionalized Porous $SiO_2$ as Heterogeneous Catalysts for Microwave Depolymerization of PET and PLA

Éadaoin Casey[1,2], Rachel Breen[1,2], Gerard Pareras Niell[3], Albert Rimola[3], Justin. D Holmes[1,2], Gillian Collins[1,2]*

[1] School of Chemistry, University College Cork, Cork, T12 YN60, Ireland.

[2] AMBER Centre, Environmental Research Institute, University College Cork, Cork, T23 XE10, Ireland.

[3]Departament de Química, Universitat Autònoma de Barcelona, 08193 Bellaterra, Catalonia, Spain.

## 1. Introduction

**Table S1**

| **Catalyst** | **PET:Cat** | **Conditions** | **BHET Yield %** | ***Reference*** |
|---|---|---|---|---|
| [Ch][OAc] | 5 wt% | 180 °C, 240 min | 85.2 | [1] |
| [bmim]Cl | 80 wt% | 180 °C, 480 min | 41.6 | [2] |
| Urea | 10 wt% | 180 °C, 180 min | 78 | [3] |
| [Bmim]OH | 5 wt% | 190 °C, 120 min | 71.2 | [4] |
| TBD: MSA salt | 0.5 eq | 180 °C, 120 min | 91 | [5] |
| *t*-$BuP_2$ | 2.4 wt% | 190 °C, 90 min | 92.7 | [6] |
| $[Ch]_3[PO_4]$ | 90 wt% | 120 °C, 180 min | 60.6 | [7] |
| [Ch][Gly] | 5 wt% | 150 °C, 6 h | 51 | [8] |
| TBD based protic ionic salts | 20 wt% | 190 °C, 120 min | 83.5 | *[9]* |
| cyanamide | 5 wt% | 190 °C, 150 min | 95.2 | *[10]* |

## 2. Experimental

### Chemicals

Mesoporous cellular foam (MCF) $SiO_2$ was obtained from Glantreo. (APTES), N,N dicyclohexylcarbodimine (DCC), 1-ethyl-3-(3-dimethylaminopropyl) carbodiimide (EDC), dicyandiamide (DCD) , methanol, ethanol, toluene, tetrahydrofuran and ethylene glycol were all purchased from Sigma Aldrich. PET was obtained from post-consumer water bottles after lids and labels were removed. Commercial PLA was obtained from Vegware lids. The plastics were cut into 1 mm x 1 mm pieces for glycolysis and methanolysis experiments. Repeating unit of 192.68 g/mol was used as the molecular weight of PET.

### 2.1 Synthesis of $SiO_2$-DCG

In a 100 ml round bottom flask, 10 mmol of the guanidine precursor, N,N dicylcohexylcarbodimine (DCC), 1-ethyl-3-(3-dimethylaminopropyl) carbodiimide (EDC) or dicyandiamide (DCD) was dissolved in 20 ml of dry toluene under argon. 2.1 ml of 3-aminopropyltriethoxylsilane (APTES) was added, and the reaction was refluxed at 100 °C for 24 h under Ar. Next 1 g of $SiO_2$ was added and the reaction was left to refluxed for a further 24 h. When the reaction had completed, the resulting mixture was filtered and washed with copious amounts of ethanol and the product and dried at 60°C in an oven.

### 2.2 Thermal glycolysis of PET

In a typical procedure, 1 g of PET, 0.1 g catalyst and 5 ml of ethylene glycol were refluxed at 190 °C for 3 h. The mass of catalyst refers to the mass of the SiO2 and the guanidine ligand, which is equivalent 2 wt% with respect to the guanidine. Once reaction was complete, 5 ml of ice-cold $H_2O$ was added to the reaction, filtered off and dried. The catalyst was separated by filtration. The filtrate was placed in the fridge overnight after which the BHET crystallised out the solution. The BHET crystals were

collected be filtration, washed with water and dried overnight before being weighed to calculate the % yield. PET conversion and yield were calculated by the equations below.

% Conversion of PET: $\frac{W_0 - W_1}{W_0} x\ 100$ **eqn. 1**

Where $W_0$ is the initial weight of the PET used and $W_1$ is the weight of the unreacted PET after the reaction.

% Yield of BHET: $\frac{W_{BHET}/M_{BHET}}{W_0/M_{PET}} x\ 100$ **eqn. 2**

Where, $W_{BHET}$ is weight of the BHET product after recrystallisation, $M_{BHET}$ is the molecular weight of BHET, $W_0$ is the initial weight of PET used and $M_{PET}$ is the repeating unit of PET (192.68 g/mol).

**2.3 Microwave assisted glycolysis of PET**

Initial MW assisted reaction were carried out under the same conditions as the thermally heated reactions, followed by an optimization study as detailed in Table S3. Optimal conditions were found to be 1 g of PET, 0.1 g catalyst and 10 ml ethylene glycol were added to the Milestone Flexiwave SK-15 high pressure digestion rotors and the reactions were carried out at between 10-60 min ranging from 190-220 °C with a stir speed of 960 rpm, ramp time of 5 min and at 800 W. The recrystallization step post-reaction was the same as for thermal glycolysis.

**2.4 Methanolysis of PLA**

0.5 g PLA, 50 mg catalyst, 5 ml MeOH and 7.5 ml of tetrahydrofuran (THF) was placed in an autoclave and sealed tight, which was then placed into oven at 130 °C for 20 h. Once reaction was complete, the resulting mixture was filtered and washed with excess MeOH, and the solvent was removed via rotary evaporation leaving the product MeLa. The unreacted plastic was collected from the filter paper, dried and weighed to calculate the PLA mass loss.

**2.5 Microwave assisted methanolysis of PLA**

0.5 g PLA, 50 mg catalyst, and a ratio of 2:3 methanol : THF were added to Teflon tubes and reacted in a Flexiwave microwave at 130 °C with a ramp time of 5 min for times ranging from 10-60 min and at 800 W.

% Conversion of PLA: $\frac{W_0 - W_1}{W_0} x\ 100$ **eqn. 3**

Where $W_0$ is the initial weight of the PLA used and $W_1$ is the weight of the unreacted PLA after the reaction.

## 3. Materials Characterisation

Scanning electron microscopy (SEM) was performed using a FEI Quanta 650 SEM at an accelerating voltage of 5 kV. The samples were gold coated using a Quorum 150T S magnetron sputtering system as they were non-conductive. X-ray Photoelectron Spectroscopy (XPS) was acquired using a KRATOS AXIS 165 monochromatized X-ray photoelectron spectrometer equipped with an Al Kα (hv = 1486.6 eV) X-ray source. Spectra were collected at a take-off angle of 90° and all spectra were referenced to the C 1s peak at 284.8 eV. Transmission electron microscopy (TEM) analysis was performed using a JEOL 2100 electron microscope at an operating voltage of 200 kV. Fourier transform infrared (FTIR) spectra were recorded on a Perkin Elmer Spectrum Two FT-IR Spectrometer operating in the range of 4000-450 $cm^{-1}$ with a resolution of 4 $cm^{-1}$ and spectra were averaged from 20 scans. BET sorption analysis was performed on a Micromeritics Tristar II surface area and porosity analyser. Prior to analysis, each sample was degassed for 3 h at 400 °C and measurements were performed at -169.15 °C (77 K). The surface area was determined using the BET (Brunauer-Emmett-Teller) method. The pore volume, pore diameter and pore size distribution were determined using the BJH (Barrett-Joyner-Halenda) method.[11] Termogravimetric analysis (TGA) was carried out on a TA Instruments Thermogravimetric Analyzer TGA Q500 V20.13 Build 39. Nuclear magnetic resonance (NMR) samples

were run in deuterated chloroform ($CDCl_3$). 1H NMR spectra were recorded on Bruker Avance III 300 NMR spectrometers, in proton-coupled mode using tetramethylsilane (TMS) as the internal standard. Microwave reactions were performed in Teflon vessels in a milestone Flexiwave microwave synthesis platform with a SK-15 high pressure rotor equipped with an IR temperature sensor.

## 4. Computational details

Density functional theory (DFT) simulations were carried out using the CP2K package.[12] The mesoporous $SiO_2$ structure used in the experiments was computationally represented as a periodic amorphous silica ($SiO_2$) surface. The chosen $SiO_2$ surface presents a silanol density of 7.2 OH/nm$^2$ assuring the maximum number of Si atoms available to be functionalized in the unit cell.[13] For the initial bare $SiO_2$ surface, both internal atomic positions and cell parameters were optimized (resulting with dimensions of a=13.34 Å, b=13.73 Å and c=49.21 Å, in which the last one represents an empty space between surface replicas). The rest of the optimizations (namely, with the ligands and to simulate reactivity) were performed only relaxing the atomic positions keeping the cell parameters fixed. Geometry optimizations were carried out using the semi-local Perdew–Burke–Ernzerhof (PBEsol) functional[14], combined with a double-ζ basis set (DZVP-MOLOPT-SR-GTH gaussian basis set) for all the atom types, together with the Grimme's D3(BJ) dispersion correction to the potential energy,[15] and a cutoff set at 500 Ry for the plane wave auxiliary basis set. Core electrons were described with the Goedecker–Teter–Hutter pseudopotentials[16] and valence ones with a mixed Gaussian and plane-wave (GPW) approach.[17] Solvation effects were considered by performing single point energy calculations on the optimized systems adopting the self-consistent continuum solvation (SCCS) model as implemented in CP2K, aiming to reproduce the experimental conditions of ethylene glycol (EG) and tetrahydrofuran (THF) as solvents.[18]

Finally, to determine the nature of the stationary points of the potential energy surfaces (i.e., local minima and saddle points) the corresponding vibrational harmonic frequencies were calculated at the PBE-D3BJ/DZVP level using the finite differences method. For frequency calculations, a partial Hessian

approach was used to reduce the computational cost of the calculations and the vibrational frequencies were calculated on only on a fragment of the system that represents the most chemically relevant part, *i.e.*, the reactive atoms and the surface site.

**Table S2:** BET analysis of bare $SiO_2$, $SiO_2$-DCG, $SiO_2$-EDG and $SiO_2$-DCD catalysts.

| | **Surface Area** $m^2g^{-1}$ | **Pore diameter** (Å) | **Pore volume** $cm^3g^{-1}$ |
|---|---|---|---|
| **$SiO_2$** | 412.4 | 108 | 0.5342 |
| **$SiO_2$ -DCG** | 182.2 | 100 | 0.4247 |
| **$SiO_2$-EDG** | 101.8 | 90 | 0.4778 |
| **$SiO_2$-DCD** | 38.4 | 84 | 0.1711 |

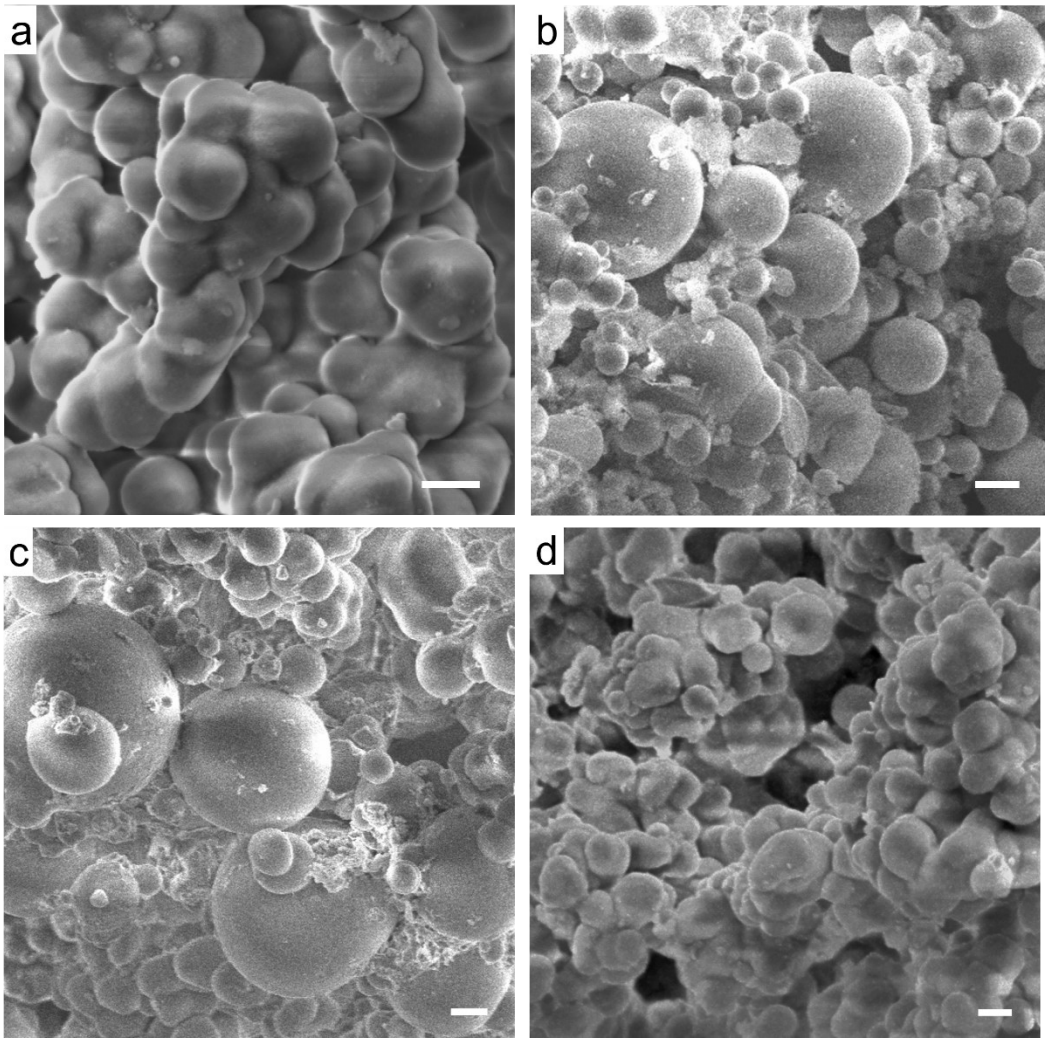



**Figure S1:** SEM images of (a) bare $SiO_2$ and after functionalization with the (b) DCG (c) EDG and (d) DCD ligands.

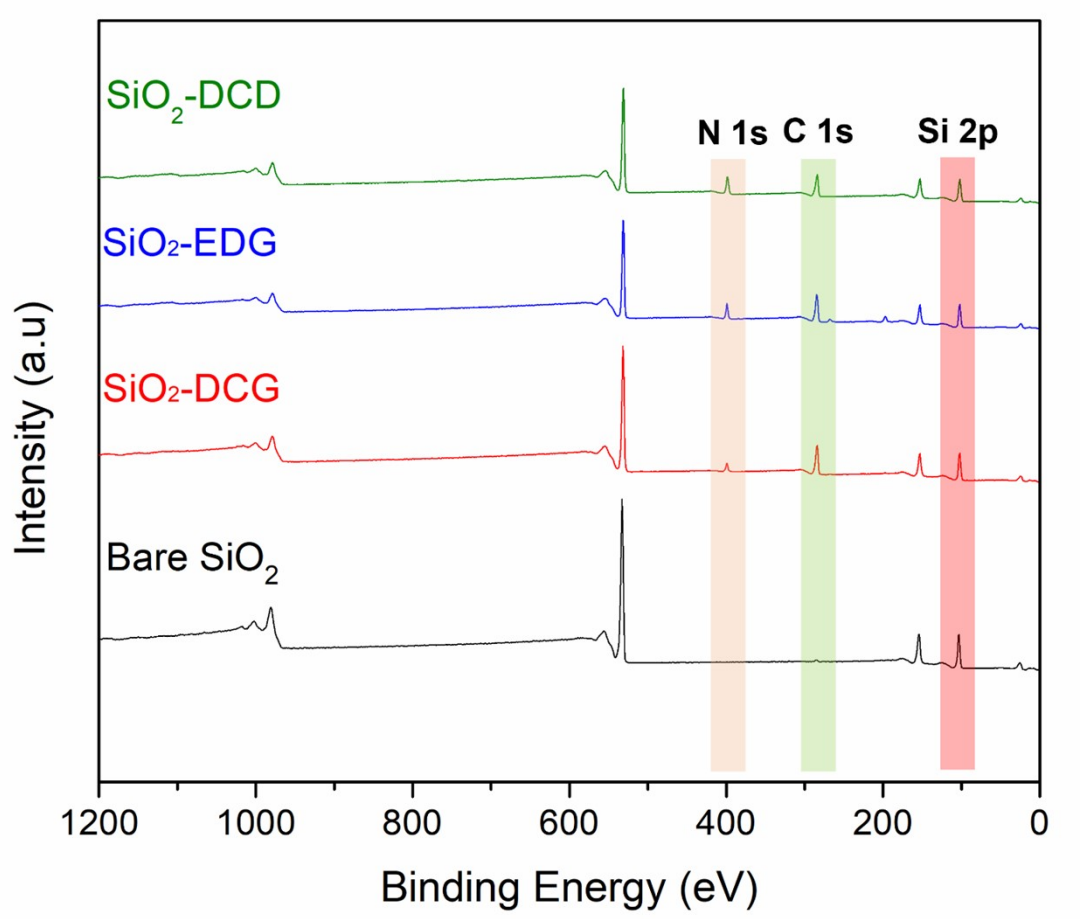



**Figure S2:** XPS Survey scan for bare $SiO_2$, $SiO_2$-DCG, $SiO_2$-EDG and $SiO_2$-DCD catalysts.

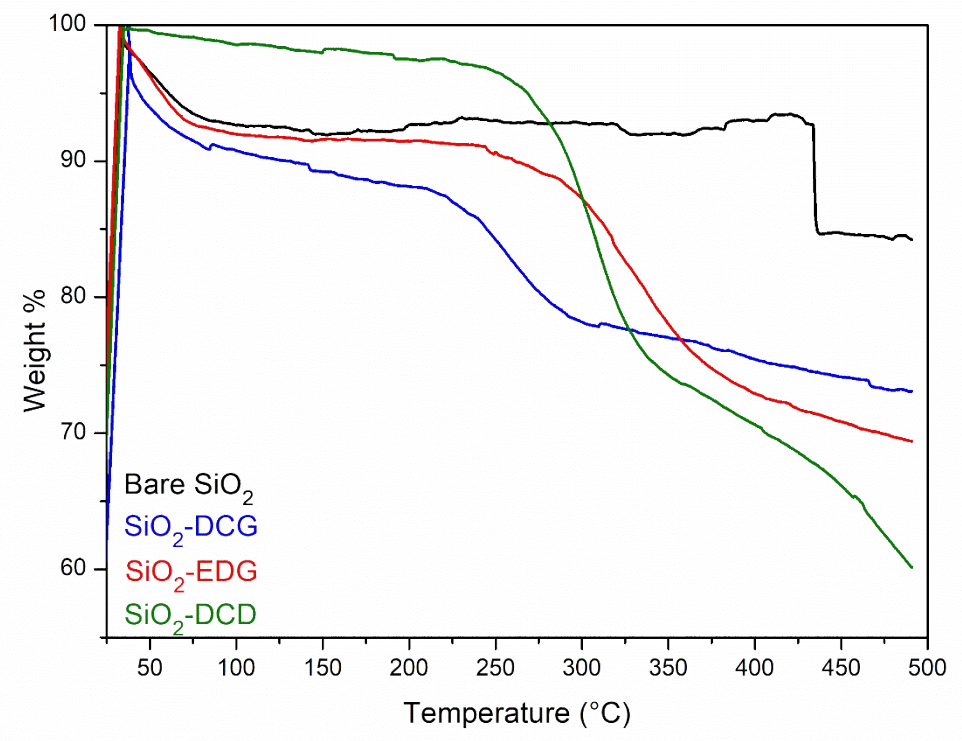



**Figure S3:** Thermogravimetric analysis of bare $SiO_2$, $SiO_2$-DCG, $SiO_2$-EDG and $SiO_2$-DCD.

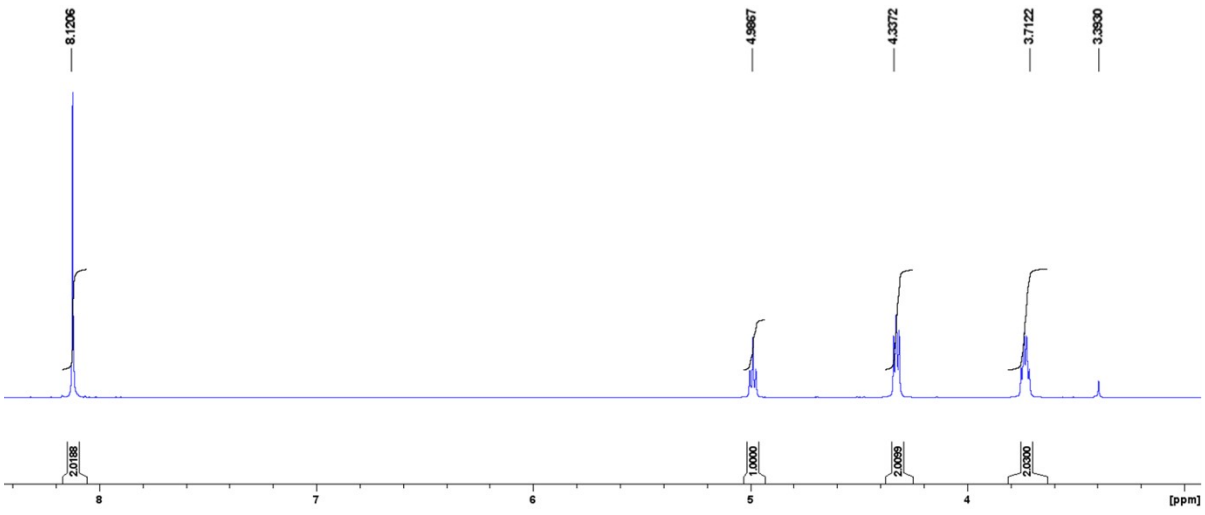



**Figure S4:** 1H NMR of the product BHET

NMR analysis confirmed that no formation of dimers or oligomers occurred and that BHET was the only product formed in the reaction. The 1H NMR spectrum of BHET can be seen in figure S5, where

the four main peaks were a singlet at 8.12 ppm corresponding to an aromatic ring, an OH triplet at 4.96 ppm, $CH_2$ triplet at 4.33 ppm and $CH_2$ quartet at 3.71 ppm. Residual solvent $d_6$-DMSO was located at 2.51 ppm. The results are in good agreement with literature values of BHET.

**Table S3:** Optimization of microwave PET depolymerization parameters.

| Catalyst | Time | Stir Speed | Temperature | Conversion PET |
|---|---|---|---|---|
| No catalyst | 40 min | 960 rpm | 190 °C | 0 % |
| No catalyst | 40 min | 960 rpm | 210 °C | 10 % |
| SiO2 (bare) | 40 min | 960 rpm | 190 °C | 10 % |
| SiO2 (bare) | 40 min | 960 rpm | 210 °C | 30 % |
| $SiO_2$-DCG | 30 min | 960 rpm | 190 °C | 6 % |
| $SiO_2$-DCG | 30 min | 960 rpm | 200 °C | 20 % |
| $SiO_2$-DCG | 30 min | 960 rpm | 210 °C | 50 % |
| $SiO_2$-DCG | 40 min | 960 rpm | 210 °C | 81 % |
| $SiO_2$-DCD | 30 min | 960 rpm | 190 °C | 23 % |
| $SiO_2$-DCD | 30 min | 960 rpm | 200 °C | 39 % |
| $SiO_2$-DCD | 30 min | 960 rpm | 210 °C | 93 % |
| $SiO_2$-DCD | 40 min | 960 rpm | 210 °C | 100 % |
| $SiO_2$-DCD | 40 min | 256 rpm | 210 °C | 85 % |
| $SiO_2$-EDG | 30 min | 960 rpm | 190 °C | 4 % |
| $SiO_2$-EDG | 30 min | 960 rpm | 200 °C | 16 % |
| $SiO_2$-EDG | 30 min | 960 rpm | 210 °C | 85 % |
| $SiO_2$-EDG | 40 min | 960 rpm | 210 °C | 100 % |

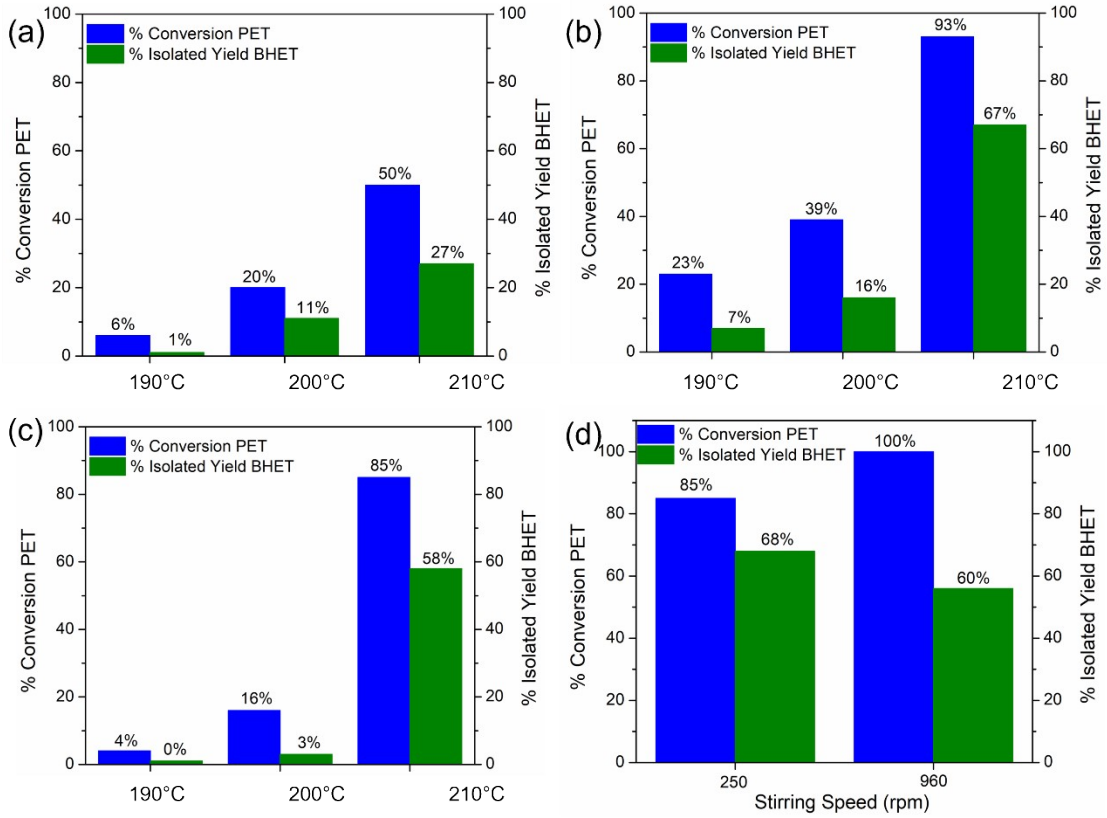



**Figure S5:** Microwave assisted glycolysis of PET under different reaction temperatures for (a) $SiO_2$-DCG, (b) $SiO_2$-EDG and (c) $SiO_2$-DCD and catalysts (d) Stir speed optimization.

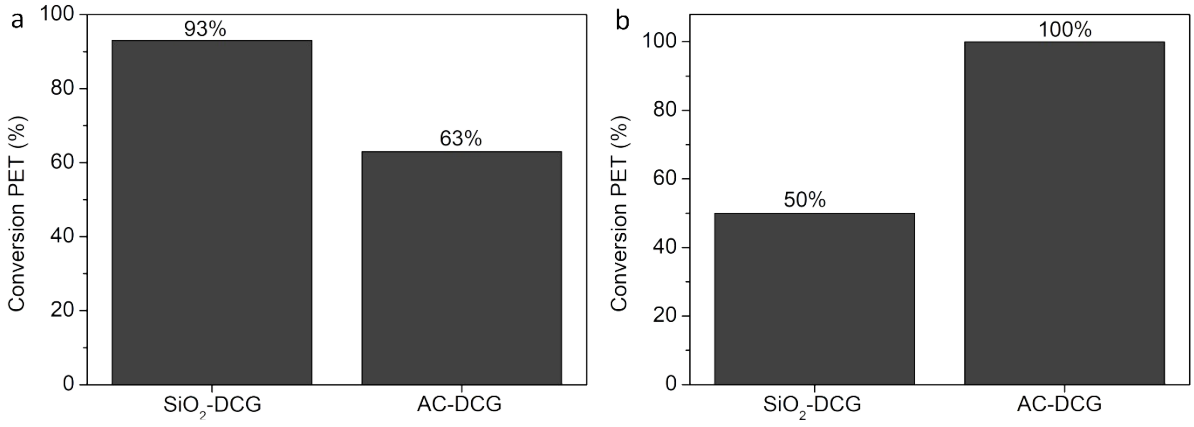



**Figure S6:** Comparison of PET glycolysis using DCG ligands supported on activated carbon and $SiO_2$ using a) conventional heating at a temperature of 190 °C and b) microwave-assisted heating at a temperature of 210 °C.

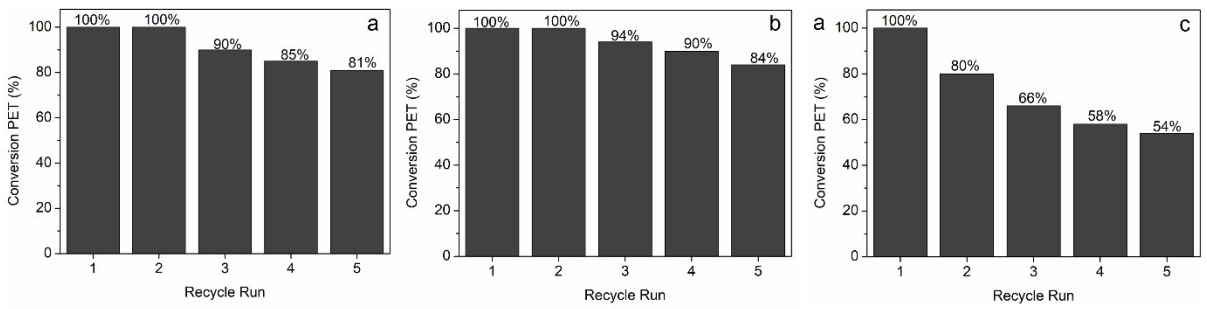



**Figure S7:** Recyclability performance of the $SiO_2$-DCD catalyst under optimised thermal conditions and (b) optimised MW conditions (c) $SiO_2$-DCG catalyst under thermal conditions.

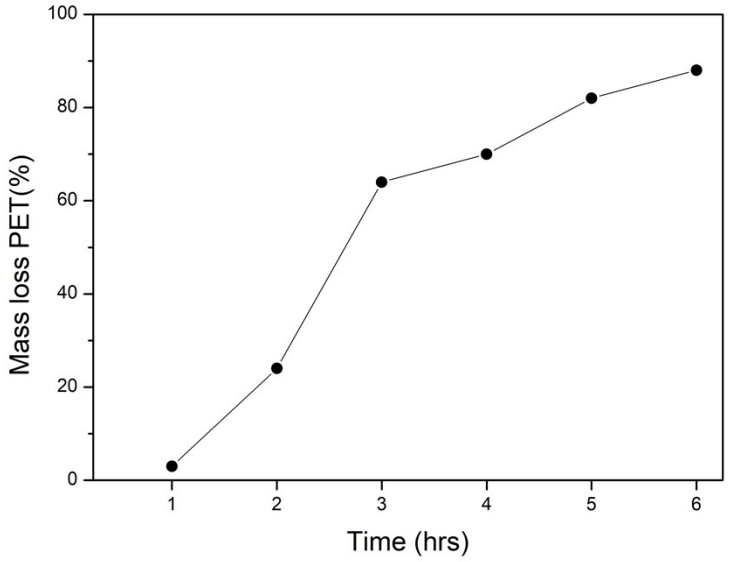



**Figure S8:** Time series of mass loss PET using 1,4 butanediol as a solvent.

**Table S4:** Reaction optimization of methanolysis of PLA under microwave irradiation.

| Catalyst | MeOH | THF | Temp | Time | Stirring | Mass Loss PLA | Oligomers | MeLa |
|---|---|---|---|---|---|---|---|---|
| EDG | 2 ml | 3 ml | 80 °C | 30 min | 256 rpm | 0 % | - | - |
| DCD | 2 ml | 3 ml | 80 °C | 30 min | 256 rpm | 35 % | - | - |
| DCG | 2 ml | 3 ml | 80 °C | 30 min | 960 rpm | 14 % | - | - |
| EDG | 2 ml | 3 ml | 80 °C | 30 min | 960 rpm | 5 % | - | - |
| DCD | 2 ml | 3 ml | 80 °C | 30 min | 960 rpm | 7 % | - | - |
| DCG | 5 ml | - | 130 °C | 30 min | 960 rpm | 96 % | 100 % | trace |
| DCG | 2 ml | 3 ml | 130 °C | 30 min | 960 rpm | 96 % | 100 % | trace |
| DCG | 1 ml | 4 ml | 130 °C | 30 min | 960 rpm | 91 % | 100 % | trace |

| | | | | | | | | |
|---|---|---|---|---|---|---|---|---|
| EDG | 2 ml | 3 ml | 130 °C | 30 min | 960 rpm | 84 % | 100 % | - |
| DCG | 2 ml | 3 ml | 130 °C | 30 min | 960 rpm | 100 % | 70 % | 30% |
| DCD | 2 ml | 3 ml | 130 °C | 30 min | 960 rpm | 97 % | 70 % | 12 % |
| DCG | 2 ml | 3 ml | 130 °C | 90 min | 960 rpm | 100 % | 68 % | 30% |

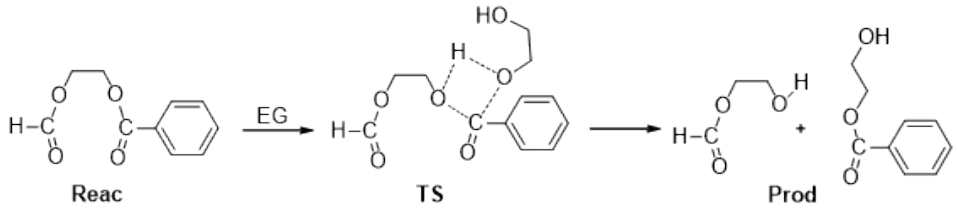
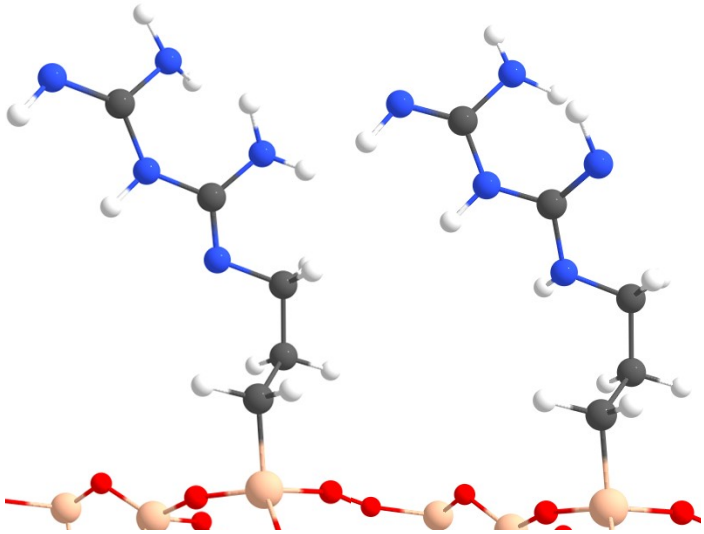



**Figure S9**. Reaction model used for the benchmarking study.

**Table S5.** Computed relative energies (in kcal $mol^{-1}$) for the reaction model used in the benchmarking study. Optimized geometries were carried out at PBE-D3(BJ)/DZVP theory level and single point energy calculations at DLPNO-CCSD(T). In parenthesis, the relative error (in %) for the potential energy barrier is also shown.

| System | PBE/DZVP | DLPNO-CCSD(T) |
|---|---|---|
| Reac | 0.00 | 0.00 |
| TS | 36.05 | 37.79 (4.6%) |
| Prod | -7.22 | -5.36 |



**(a)** **(b)**

**Figure S10 (a):** Optimized structure for the $SiO_2$-DCD tautomer with one primary amine, two secondary amine and two imines. **(b)** Optimized structure for the DCD@$SiO_2$ tautomer with two primary amines, one secondary amine and two imines. Colour scheme: grey for C, red for O, white for H, blue for N and beige for Si.

**Table S6.** Collected the relative Gibbs energies at 190 °C in kcal $mol^{-1}$ for the uncatalyzed PET depolymerization reaction considering 1, 2, 3 and 4 units of ethylene glycol (EG) involved in the transition state.

| **System** | **1 EG** *kcal mol$^{-1}$* | **2 EG** *kcal mol$^{-1}$* | **3 EG** *kcal mol$^{-1}$* | **4EG** *kcal mol$^{-1}$* |
|---|---|---|---|---|
| 1 | 0.00 | 0.00 | 0.00 | 0.00 |
| $TS_{1-2}$ | 24.26 | 19.29 | 17.06 | 16.43 |
| 2 | 12.82 | 12.82 | 12.82 | 12.82 |


1. Y. Liu, X. Yao, H. Yao, Q. Zhou, J. Xin, X. Lu and S. Zhang, *Green Chemistry*, 2020, **22**, 3122-3131.
2. H. Wang, Y. Liu, Z. Li, X. Zhang, S. Zhang and Y. Zhang, *European Polymer Journal*, 2009, **45**, 1535-1544.
3. Q. Wang, X. Yao, S. Tang, X. Lu, X. Zhang and S. Zhang, *Green Chemistry*, 2012, **14**, 2559-2566.
4. Q. F. Yue, C. X. Wang, L. N. Zhang, Y. Ni and Y. X. Jin, *Polymer Degradation and Stability*, 2011, **96**, 399-403.
5. C. Jehanno, I. Flores, A. P. Dove, A. J. Müller, F. Ruipérez and H. Sardon, *Green Chemistry*, 2018, **20**, 1205-1212.
6. C. Fan, L. Zhang, C. Zhu, J. Cao, Y. Xu, P. Sun, G. Zeng, W. Jiang and Q. Zhang, *Green Chemistry*, 2022, **24**, 1294-1301.
7. J. Sun, D. Liu, R. P. Young, A. G. Cruz, N. G. Isern, T. Schuerg, J. R. Cort, B. A. Simmons and S. Singh, *ChemSusChem*, 2018, **11**, 781-792.
8. S. Marullo, C. Rizzo, N. T. Dintcheva and F. D'Anna, *ACS Sustainable Chemistry & Engineering*, 2021, **9**, 15157-15165.
9. C. Zhu, L. Yang, C. Chen, G. Zeng and W. Jiang, *Physical Chemistry Chemical Physics*, 2023, **25**, 27936-27941.
10. Z. Wang, Y. Jin, Y. Wang, Z. Tang, S. Wang, G. Xiao and H. Su, *ACS Sustainable Chemistry & Engineering*, 2022, **10**, 7965-7973.
11. S. Brunauer, P. H. Emmett and E. Teller, *Journal of the American Chemical Society*, 1938, **60**, 309-319.

12. J. Hutter, M. Iannuzzi, F. Schiffmann and J. VandeVondele, *WIREs Computational Molecular Science*, 2014, **4**, 15-25.
13. P. Ugliengo, M. Sodupe, F. Musso, I. J. Bush, R. Orlando and R. Dovesi, *Advanced Materials*, 2008, **20**, 4579-4583.
14. J. P. Perdew, A. Ruzsinszky, G. I. Csonka, O. A. Vydrov, G. E. Scuseria, L. A. Constantin, X. Zhou and K. Burke, *Physical Review Letters*, 2008, **100**, 136406.
15. S. Grimme, J. Antony, S. Ehrlich and H. Krieg, *The Journal of Chemical Physics*, 2010, **132**.
16. S. Goedecker, M. Teter and J. Hutter, *Physical Review B*, 1996, **54**, 1703-1710.
17. G. Lippert, J. Hutter and M. Parrinello, *Molecular Physics*, 1997, **92**, 477-488.
18. O. Andreussi, I. Dabo and N. Marzari, *The Journal of Chemical Physics*, 2012, **136**.